

# Optical shaping of high-pressure gas-jet targets for proton acceleration experiments in the near-critical density regime

I. Tazes<sup>1,2</sup>, G. Andrianaki<sup>1,4</sup>, A. Grigoriadis<sup>1,5</sup>, S. Passalidis<sup>6</sup>, A. Skoulakis<sup>1</sup>, E. Kaselouris<sup>1</sup>, E. Vrouvaki<sup>1,2</sup>, J. Chatzakis<sup>1,2</sup>, I. Ftilis<sup>1,2</sup>, M. Bakarezos<sup>1,3</sup>, E.P. Benis<sup>1,5</sup>, V. Dimitriou<sup>1,3</sup>, N.A. Papadogiannis<sup>1,3</sup> and M. Tatarakis<sup>1,2</sup>

<sup>1</sup>*Institute of Plasma Physics & Lasers - IPPL, Hellenic Mediterranean University Research Centre, Rethymnon, Greece*

<sup>2</sup>*Department of Electronic Engineering, Hellenic Mediterranean University, Chania, Greece*

<sup>3</sup>*Department of Music Technology and Acoustics, Hellenic Mediterranean University, Rethymnon, Greece*

<sup>4</sup>*School of Production Engineering and Management, Technical University of Crete, Chania, Greece*

<sup>5</sup>*Department of Physics, University of Ioannina, Ioannina, Greece*

<sup>6</sup>*Sorbonne Université, CNRS, Laboratoire de Chimie Physique-Matière et Rayonnement, Paris, France*

## Abstract

Laser-induced proton acceleration is a subject of great interest due to its numerous potential applications, among others in energy production through Inertial Confinement Fusion (ICF), or in medical applications such as hadron therapy. Extreme pressure gas-jet targets, able to reach the near-critical density (NCR) regime, can be used as high repetition rate (HRR), debris-free proton sources. In the near-critical regime, Magnetic Vortex Acceleration (MVA) is one of the most promising proton acceleration mechanisms. While state-of-the-art simulations predict hundreds of MeV of protons by super-intense, short wavelength, femtosecond laser pulses, MVA remains experimentally challenging due to the extremely steep density gradient plasma profiles required as implied by simulations. Here, we present Magnetohydrodynamic (MHD) simulations results on the capability of delivering optically shaped targets through the interaction of nanosecond laser pulses with high-density gas-jet profiles. Multiple laser-generated Blast Wave (BW) schemes capable to compress the gas target into near-critical steep density gradient slabs of few microns thickness are reported. In addition, experimental findings of the optically shaped gas-jet targets, delivered by a solenoid valve along with an air-driven hydrogen gas booster, able to support 1000 bar of backing pressure are presented [1]. Additionally, the capability of proton acceleration by the interaction of the compressed, steep gradient, near-critical density developed targets, with the fs laser pulse of the ZEUS 45TW laser system of IPPL, is demonstrated by 3D Particle-In-Cell (PIC) simulations.

Up to date, protons of  $\sim 100$  MeVs are generated, using solid targets, by the Target Normal Sheath Acceleration (TNSA) mechanism [2,3]. In TNSA, the solid targets are destroyed upon irradiation and need to be replaced after each laser shot, not allowing the possibility of HRR proton sources. High-pressure gas targets are considered a promising alternative which can support HRR, debris-free proton sources [4,5]. Protons and ions up to 20 MeV per nucleon [6] have been experimentally accelerated by MVA [7], using ns CO<sub>2</sub> lasers, that can access the NCR regime at low densities (critical density  $n_{cr} \approx 10^{19}$  electrons/cm<sup>-3</sup>) due to their long wavelengths ( $\lambda \approx 10$   $\mu$ m). State-of-the-art simulations predict hundreds of MeV of protons by super-intense, fs, Ti:Sa laser systems, although extremely high densities, of the order of  $n_{cr} \approx 10^{21}$  electrons/cm<sup>-3</sup>, are required due to their short-wavelength ( $\lambda \approx 0.8$   $\mu$ m).

In this work, we study the optical shaping of gas-jet profiles via multiple Sedov type, colliding BWs, to generate NCR ( $0.1n_{cr} - 10n_{cr}$ ), sharp, target profiles [7,8], optimized for proton acceleration experiments, using the 45 TW, Ti:Sa ZEUS laser system of IPPL [1,3]. The evolution of the BWs is simulated using the MHD code FLASH [10]. The proton acceleration efficiency is demonstrated by PIC simulations using the code EPOCH [11].

The 3D Gaussian gas-jet profile with  $n = n_0 e^{-\frac{1}{300 \times 10^{-6}}(x^2 + 0.2y^2 + z^2)}$ , is initially irradiated by a 835 mJ, 6ns, Nd:YAG laser pulse at X, Y, Z = 0, 250, 120  $\mu$ m. The initial gas-jet density at the region of the interaction is  $8.7 \times 10^{19}$  atoms/cm<sup>3</sup> corresponding to 5% of the critical density ( $n = 0.05n_{cr}$ ) for laser wavelength  $\lambda = 800$  nm. Figure 1 shows the temporal evolution of BW shock front while it propagates inside the gas-jet.

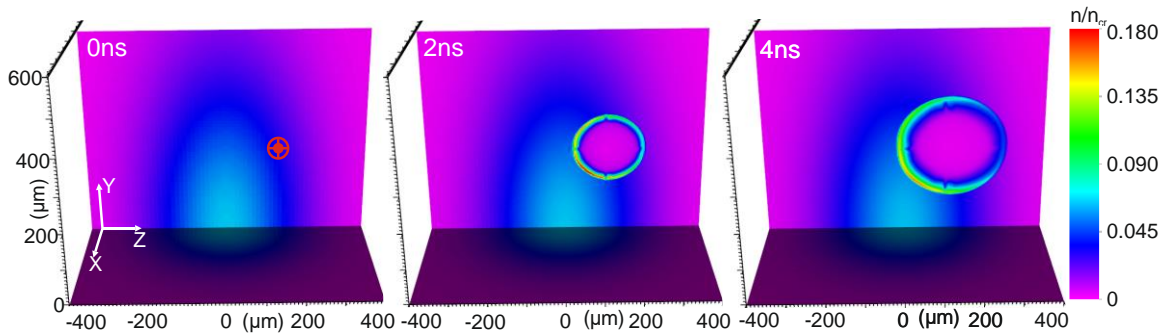


**Figure 1:** Temporal evolution of a single BW shock front inside the H gas-jet density profile. The density is given as the ration of H density over critical density  $n/n_{cr}$

A compression factor  $C=3.1$  is achieved by the BW at  $t = 2$  ns.  $C$  is defined as the ratio of the density of the gas-jet while compressed by the BW shock front over the initial density. It should be mentioned that  $C$  is close to the Strong shock limit  $c = (\gamma + 1)/(\gamma - 1)$ , which for the atomic H

( $\gamma = 1.67$ ) is  $C = 4$ . The shock front of the BW is characterized by a steep density gradient profile, with a full width at half maximum  $l_{FWHM} = 15.8 \mu\text{m}$ .

The optical shaping of the gas-jet via the collision of multiple BW shock fronts, for the generation of steeper density gradient profiles and greater compression is investigated. The ns laser pulse is split into two identical pulses of 417.5 mJ of energy each, deposited biaxially to the centre of the gas-jet for  $Y = 250 \mu\text{m}$  and  $Z = \pm 120 \mu\text{m}$ . Figure 2 shows the temporal evolution of the two counter propagating BWs inside the gas-jet. The BWs shock front collision occurs at  $t = 4 \text{ ns}$  at the centre of the gas-jet density profile.

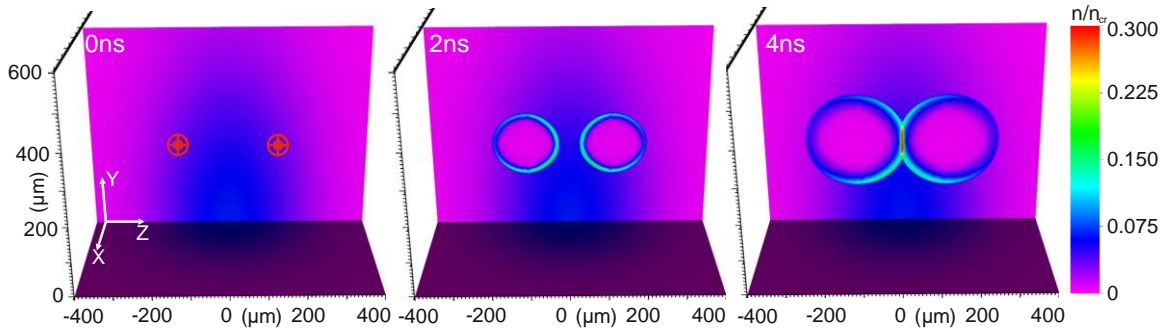


**Figure 2:** Temporal evolution of two counterpropagating BW shock fronts inside the H gas-jet density profile.

The resulting compression  $C = 6.3$  corresponds to  $n = 0.30n_{cr}$  and it is characterized by a steeper density profile with  $l_{FWHM} = 11.5 \mu\text{m}$ . Various geometrical set-ups with two or more laser pulses, to achieve steeper gradient profiles of higher level of compression, are further investigated.

The optically shaped H density profiles were implemented as initial conditions, in the PIC simulations, to demonstrate their efficiency in proton acceleration for TW-class laser systems. The 3D PIC models are developed in a computational domain of  $80 \times 40 \times 40 \mu\text{m}$  size, discretized by  $1600 \times 400 \times 400$  cells.

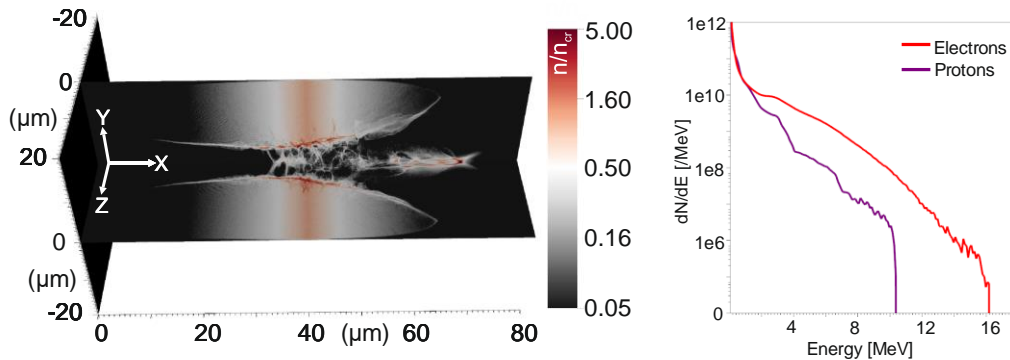


**Figure 3:** (left) ionized H density at 600 fs of the 3D PIC simulation where the MVA proton beam is demonstrated, (right) MVA particle energy spectra at 600 fs of the simulation.

Figure 3 (left) shows the ionized H density, with initial peak density  $n = n_{cr}$ , at  $t = 600$  fs of the simulation. The 45 TW accelerating laser pulse enters the computational domain at  $t = 0$  fs of the simulation. The energy spectra of the accelerated particles are demonstrated in figure 3 (right), where the proton cut-off energy is  $\sim 10$  MeV. The maximum value of MVAs typical azimuthal magnetic field [12,13], at  $\sim 200$  fs of the simulation that the laser pulse penetrates the peak density of the target, exceeds  $0.5 \times 10^5$  T.

The high-density gas-jet profiles are delivered by a Haskel air-driven hydrogen gas booster, along with a Clark Cooper Solenoid valve, able to support 1000 bar of backing pressure. Figure 4 shows a preliminary gas-jet profile delivered by a designed 400  $\mu\text{m}$  diameter conical nozzle characterized by Mach - Zehnder interferometry. The gas-jet profile corresponds to 60 bars of Nitrogen. Higher backing pressures, up to 400 bars of gas mixtures (Nitrogen – Hydrogen, Helium – Hydrogen) are planned to be performed to achieve the optimal profile for the optical shaping.

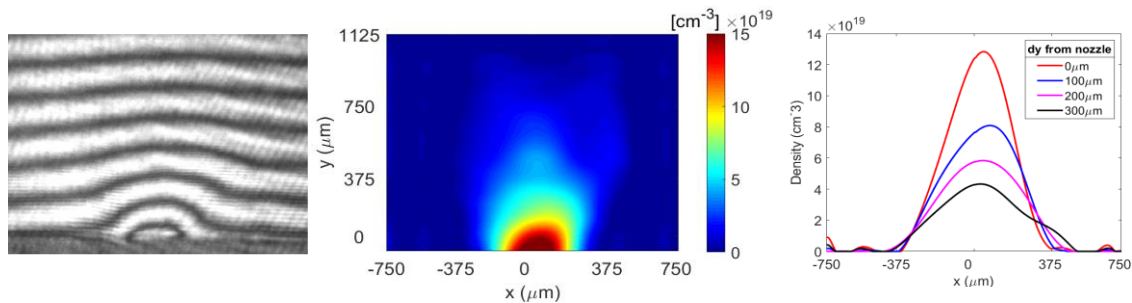


**Figure 4:** (left) signal image of the Mach - Zehnder interferometry for 60 bar Nitrogen, (middle) density derived by Abel inversion, (right) density lineouts along various distances from the nozzle tip.

## Acknowledgements

This work has been carried out within the framework of the EUROfusion Consortium, funded by the European Union via the Euratom Research and Training Programme (Grant Agreement No 101052200 — EUROfusion). Views and opinions expressed are however those of the author(s) only and do not necessarily reflect those of the European Union or the European Commission. Neither the European Union nor the European Commission can be held responsible for them.”

The simulations were performed in the National HPC facility—ARIS—using the computational time granted from the Greek Research & Technology Network (GRNET) under project ID pr011027—LaMPIOS.

## References

- [1] Clark, E. L., et al. *High Power Laser Sci. Eng.*, (2021), pp. 1–28., DOI: [10.1017/hpl.2021.38](https://doi.org/10.1017/hpl.2021.38)
- [2] Wagner, F., et al. *Phys. Rev. Lett.* 116.20 (2016): 205002. DOI: [10.1103/PhysRevLett.116.205002](https://doi.org/10.1103/PhysRevLett.116.205002)
- [3] Tazes, I., et al. *Plasma Phys. Control. Fusion* 62.9 (2020): 094005. DOI: [10.1088/1361-6587/aba17a](https://doi.org/10.1088/1361-6587/aba17a)
- [4] Sylla, F., et al. *Rev. Sci. Instrum.* 83.3 (2012): 033507. DOI: [10.1063/1.3697859](https://doi.org/10.1063/1.3697859)
- [5] Bonvalet J., et al. *Physics of Plasmas* 28, 113102 (2021). DOI: [10.1063/5.0062503](https://doi.org/10.1063/5.0062503)
- [6] Willingale, L., et al. *Phys. Rev. Lett.* 96.24 (2006): 245002. DOI: [10.1103/PhysRevLett.96.245002](https://doi.org/10.1103/PhysRevLett.96.245002)
- [7] Bulanov, S. S., et al. *Phys. Plasmas* 17.4 (2010): 043105. DOI: [10.1063/1.3372840](https://doi.org/10.1063/1.3372840)
- [8] Passalidis, S, et al *High Power Laser Sci. Eng.* 8 (2020). DOI: [10.1017/hpl.2020.5](https://doi.org/10.1017/hpl.2020.5) (and references within)
- [9] Marquès J.-R., et al. *Physics of Plasmas* 28, 023103 (2021). DOI: [10.1063/5.0031313](https://doi.org/10.1063/5.0031313) (and references within)
- [10] [http://flash.uchicago.edu/site/flashcode/user\\_support/flash4\\_ug\\_4p3.pdf](http://flash.uchicago.edu/site/flashcode/user_support/flash4_ug_4p3.pdf)
- [11] Arber, T. D., et al. *Plasma Phys. Control. Fusion* 57.11 (2015): 113001. DOI: [10.1088/0741-3335/57/11/113001](https://doi.org/10.1088/0741-3335/57/11/113001)
- [12] Nakamura, T., et al. *Physical review letters* 105.13 (2010): 135002. DOI: [10.1103/PhysRevLett.105.135002](https://doi.org/10.1103/PhysRevLett.105.135002)
- [13] Park J., et al. *Physics of Plasmas* 26.10 (2019): 103108. DOI: [10.1063/1.5094045](https://doi.org/10.1063/1.5094045)